J. Micromech. Microeng. **20** (2010) 055001 (9pp) doi:10.1088/0960-1317/20/5/055001

# Straight SU-8 pins

**R Safavieh, M Pla Roca, M A Qasaimeh, M Mirzaei and D Juncker**

Biomedical Engineering Department and Genome Quebec Innovation Centre, McGill University, Montreal, Canada

E-mail: david.juncker@mcgill.ca

Received 24 November 2009, in final form 9 February 2010
Published 23 March 2010
Online at stacks.iop.org/JMM/20/055001

**Abstract**

SU-8 can be patterned with high resolution, is flexible and tough. These characteristics qualify SU-8 as a material for making spotting pins for printing DNA and protein microarrays, and it can potentially replace the commonly used silicon and steel pins that are expensive, brittle in the case of silicon and can damage the substrate during the printing process. SU-8, however, accumulates large internal stress during fabrication and, as a consequence, thin and long SU-8 structures bend and coil up, which precludes using it for long, freestanding structures such as pins. Here we introduce (i) a novel fabrication process that allows the making of 30 mm long, straight spotting pins that feature (ii) a new design and surface chemistry treatments for better capillary flow control and more homogeneous spotting. A key innovation for the fabrication is a post-processing annealing step with slow temperature ramping *and* mechanical clamping between two identical substrates to minimize stress buildup and render it symmetric, respectively, which together yield a straight SU-8 structure. SU-8 pins fabricated using this process are compliant and resilient and can buckle without damage during printing. The pins comprise a novel flow stop valve for accurate metering of fluids, and their surface was chemically patterned to render the outside of the pin hydrophobic while the inside of the slit is hydrophilic, and the slit thus spontaneously fills when dipped into a solution while preventing droplet attachment on the outside. A single SU-8 pin was used to print 1392 protein spots in one run. SU-8 pins are inexpensive, straightforward to fabricate, robust and may be used as disposable pins for microarray fabrication. These pins serve as an illustration of the potential application of ultralow stress SU-8 for making freestanding microfabricated polymer microstructures.

S Online supplementary data available from stacks.iop.org/JMM/20/055001/mmedia

## 1. Introduction

The negative tone epoxy photoresist EPON SU-8 can readily be patterned with aspect ratios as high as 20, and with thickness varying from nanometers to 1 mm [1]. SU-8 has been used for making a wide variety of devices, including cantilever-based biosensors [2, 3], low-cost point-of-care diagnostics [4, 5] and microvalves [6]. One of the major drawbacks of SU-8 is its high residual stress, which leads to bending of the microstructures [7, 8] caused by the mismatch between the thermal expansion coefficients of SU-8 and the substrate.

Many approaches have already been developed to reduce the residual stress in SU-8. One efficient way is to use an adaptive layer made of polymers such as polyethylene terephtalate (PET) [8] or polystyrene [9] that have an expansion coefficient similar to SU-8. These adaptive layers also act as release layers, which can be dissolved and allow detaching of the SU-8 structures without resorting to mechanical force [9, 10]. Similarly, SU-8 itself can be used as an adaptive layer by evaporating a protective layer of metal (i.e. gold or chromium) on top. The sacrificial SU-8 layer is shielded from UV light and from being cross-linked by the metal, and can thus be dissolved at the end of the process, leaving freestanding structures [11]. Another approach is to modify the baking parameters [8–10, 12, 13] and specifically reduce the temperature of the pre-bake. A lower pre-bake temperature results in a higher residual solvent content, which leads to increased mobility of monomers that in turn allow lowering the post-bake temperature and thus the overall stress is reduced [13]. A drawback of this method is a high residual solvent content which tends to evaporate subsequently and lead stress buildup, which is what we observed as part of

 

our experiments and describe in the results section. Whereas these strategies help reduce the residual stress and bending by orders of magnitude, the distortion still remains significant. Due to these issues, SU-8 has not yet been used for making thin, long freestanding and straight structures, such as pins for microarray spotting, to the best of our knowledge.

Pin spotting (or printing) is the original method developed for patterning biomolecules such as DNA and proteins as microarrays and is still widely used due to its ease of operation [14]. The idea of robotized pin spotting was introduced as early as 1996 for making DNA microarrays [15]. In protein microarrays, antibodies or purified proteins are microarrayed instead of DNA. Antibody microarrays are used analogously to DNA microarrays to measure the concentration of tens or hundreds of proteins at once from minute amounts of (crude) sample by measuring the fluorescent intensity on each spot [16]. Pin spotting operates by first dipping an array of pins in a 96 or 384 microtiter well plate containing spotting solutions, retracting it along with a small droplet of solution captured by capillary effects on each pin, or inside the slit if there is one, and then printing the pin array onto a surface, thus affecting the transfer of the solution from the pin to the surface. The transfer of liquid is a result of the balance between the capillary retention of the pin and the capillary effects resulting from the dynamic contact between the pin and the substrate; a microscopic gap is formed immediately before and after the contact between the pin and the substrate, and it draws liquid onto the surface. Scaling is easy for contact printing and print heads with 96 pins are common, and heads with up to 192 pins have been produced [17], which is much larger than for bioinkjet printers that are limited to 16 or 32 heads. The scalability stems from the fact that loading and spotting operate using capillary effects so that a single functional pin can be cloned and used as part of an array of pins with identical properties for each one.

Many different pin designs have been developed ranging from simple needles with a blunt tip useful for a few spotting cycles only to pins with slit and reservoirs that can be used to print hundreds of spots following a single dip loading [14]. Pins are traditionally made out of stainless steel, tungsten and titanium, and are manufactured serially using techniques such as sawing, grinding, electric discharge machining (EDM) and laser machining [14, 15]. Ceramic pins and microcapillaries [18] have also been made and shown to be more durable and less susceptible to tapping forces, while improving the spot morphology and consistency [19]. However, both for metal and ceramic pins, the fabrication remains time-consuming and cost intensive.

More recently, Si pins have been introduced. These pins can be fabricated by batch processing using micromachining techniques such as deep reactive ion etching. When using Si, much higher resolution can be achieved, and much smaller pins can be made which can be arrayed at a much higher density, up to one pin every 2.25 mm (which is the same spacing as in a 1536 microtiter well plate) [17]. However, the Si pins remain expensive, because costly deep reactive ion etchers are needed, and they need to be etched through a wafer, further entailing long fabrication time. Another drawback of Si is that it is a brittle material, and consequently, the pins break easily during manipulation and the tips rapidly deteriorate and lose their functionality. Si pins therefore need to be replaced regularly. In addition, another important issue with these pins is droplets sticking on the outside of the pins, which is more pronounced with rectangular silicon pins compared to the rounded steel pins [20].

One of the major issues with the usage of pins is that the contact between the pin and the substrate can lead to an inhomogeneous spreading of the sample. Spot homogeneity still remains a challenge despite many years of work on pins and is difficult to control, as it depends not only on the geometry of the pin itself, but also on its surface chemistry, on capillary effects and can vary as a function of the number of printing cycles. In particular, the first spots tend to be larger than the later ones as the solution is used up.

Polymer materials have not been used for fabricating pins despite the fact that they are inexpensive, tough and therefore likely to sustain many printing cycles. An important reason is that polymers are difficult to structure at the microscale with the high aspect ratios needed for making spotting pins, with the notable exception of SU-8, but it suffers from high internal stress.

In this paper, we present a novel fabrication process with an annealing step for making long, thin freestanding SU-8 structures that are straight over a length of 30 mm without measurable bending as assessed by optical microscopy. This process is used to make SU-8 pins with an improved design, including a novel capillary stop valve that allows precise metering of the sample. We also introduce surface patterning of pins by microcontact printing of hydropbobic and hydrophilic thiols on the rectangularly shaped pins. We illustrate the resilience of SU-8 pins by reversible buckling, and assess their spotting performance by testing the number of spots that can be produced and by measuring the homogeneity of a microarray of spots.

## 2. Design of the pins

The pins need to be inserted into a commercial pin holder (see figure S1 in the supplementary materials, available at stacks.iop.org/JMM/20/055001/mmedia) with collimators that serve to align the pins and are made for pins that are 200 $\mu$m thick and 1 mm wide, and which impose the width and thickness of the pins [17]. The length of the pins was chosen to be 30 mm, which is needed to reach the bottom of the wells of microtiter plates for loading liquids. The design is shown in figure 1.

The pins can be divided into three functional parts. The first one is the tip, which comes in contact with the substrate and controls the size of the spots; the second one is the slit, which acts as a microfluidic reservoir and a capillary pump; and the third part is a 'bubble' with a stop valve, which is used to precisely control the amount of liquid loaded into the pin. The basis for our design was the use of pins commercially distributed by parallel synthesis [17]. The main changes are the bubble geometry, surface chemistry and material used, all of which contribute to added functionality.

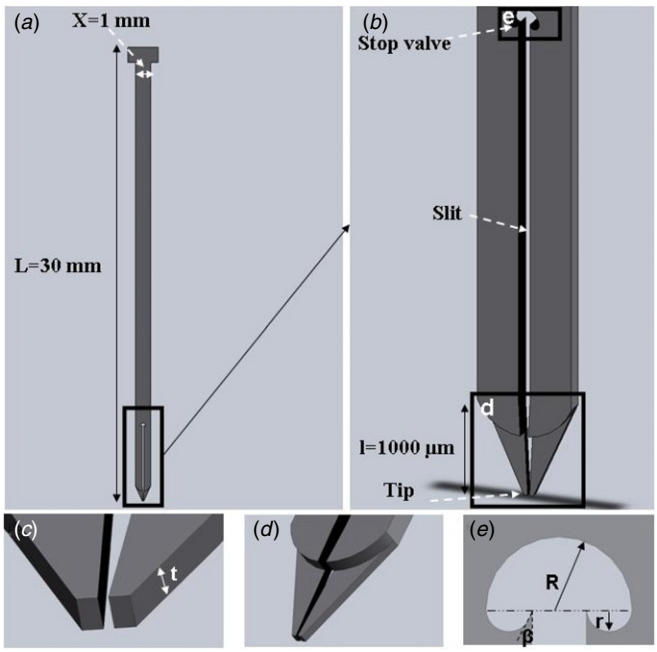


**Figure 1.** Design features and dimensions of the pin. (*a*) Overview of the pin and (*b*) view of the tip, slit and the stop valve. (*c*) Enlarged view of the tip of the pin and (*d*) featuring the (two) layers of the pins. (*e*) Bubble with a capillary stop valve, which was designed to stop the liquid at the end of the microchannel; $R = 200$ $\mu$m is the radius of curvature in the top part of the stop valve, $r = 50$ $\mu$m is the radius of curvature in the bottom part of the stop valve and $\beta$ is the angle at the interface between the channel and the bubble, which makes the liquid stop at the end of the channel.

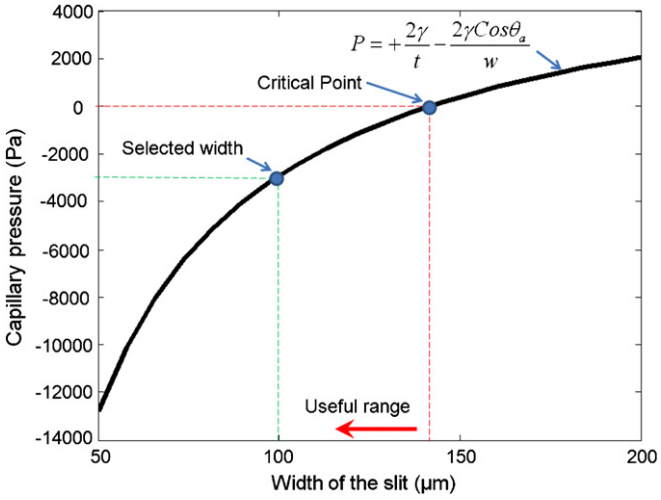


**Figure 2.** Capillary pressure of the liquid as a function of the width $w$ of the slit for a constant thickness $t = 200$ $\mu$m and a liquid–solid contact angle $\theta_a = 45^\circ$. The capillary pressure is negative for $w < 141$ $\mu$m, and consequently, the liquid will fill the microchannel. A width of 100 $\mu$m (corresponding to an aspect ratio of 2:1) was selected for the slit to provide both a high capillary pressure and sufficient volume.

### *2.1. Tip*

The size of the tip is determined by the thickness of the tip and its width, which in turn controls the size of the spot deposited on the surface. The pin consists of one or two layers (figure 1(*d*)), where the first layer controls the 'height' of the spots, $t$, and the two layers together make up 200 $\mu$m in thickness, which is imposed by the size of the collimator. When making 200 $\mu$m spots, a single layer is suitable; however, for spot sizes less than 200 $\mu$m, two-layer pins are needed. A tip with a square cross-section of 100 $\times$ 100 $\mu$m$^2$ leads to a spot with a rounded square shape having a diameter of 140 $\mu$m.

### *2.2. Slit*

For spontaneous filling of the microfluidic channel, there needs to be a free energy gain. The increase of solid–liquid interface during filling (energy gained) needs to compensate for the increase in the liquid–air interface (energy lost) in the slit. Expressed differently, the capillary pressure at the filling front in the slit needs to be negative. For pins with a slit (capillary gap) of width $w$ and a depth $t$, and an advancing contact angle between the solid–liquid interface in the microchannel, $\theta_a$, the governing equation for the total pressure of the liquid in the pin's slit can be written as follows [21]:

$$P = +\frac{2\gamma}{t} - \frac{2\gamma \cos\theta_a}{w} + \rho g h < 0. \qquad (1.1)$$

For a capillary slit with a maximal length of 7 mm, as is the case here, the hydrodynamic pressure difference due to the gravity is $\Delta P = 70$ Pa and can be neglected when compared to the capillary pressure. The pressure in the liquid depends on the width of the slit and on the aspect ratio, $t/w$. By decreasing the aspect ratio, the capillary pressure decreases and when the ratio of the thickness, $t$, to the width, $w$, approaches 1, filling becomes conditional on having contact angles very close to 0°, and turns into energetically unfavorable under all circumstances for $t \geqslant w$. Using a design similar to the one proposed here, the thickness of the slit is $t = 200$ $\mu$m, water was assumed as a working medium with $\gamma = 70$ mN m$^{-1}$, and $\theta_a = 45^\circ$ [22]. Under these conditions, $\Delta P < 0$ for $w < 141$ $\mu$m, and the liquid will fill the slit spontaneously. Figure 2 shows the capillary pressure of the liquid as a function of the width $w$ of the slit. In order to ensure robust filling of the pins and provide a sufficient volume, $w$ was set to 100 $\mu$m. Close to the tip, where the thickness and the width of the pin are reduced, $w$ narrows down as well, but since the tip is the last to be drained, it does not affect the capillary pressure during spotting.

In addition, we estimated the elastic deformation of the tip of the pins due to the capillary pressure, which after filling may lead to bending of the tips, if the pins are too soft. For SU-8, which has an elastic modulus of 5.25–6.21 GPa [23], the tip deflection is only about 1 $\mu$m for a pin that has 7 mm long prongs (see figure S2 in the supplementary materials, available at stacks.iop.org/JMM/20/055001/mmedia). This value is negligible in practice for the slit sizes of 100 $\mu$m and will not influence the capillary transfer from the pin to the substrate.

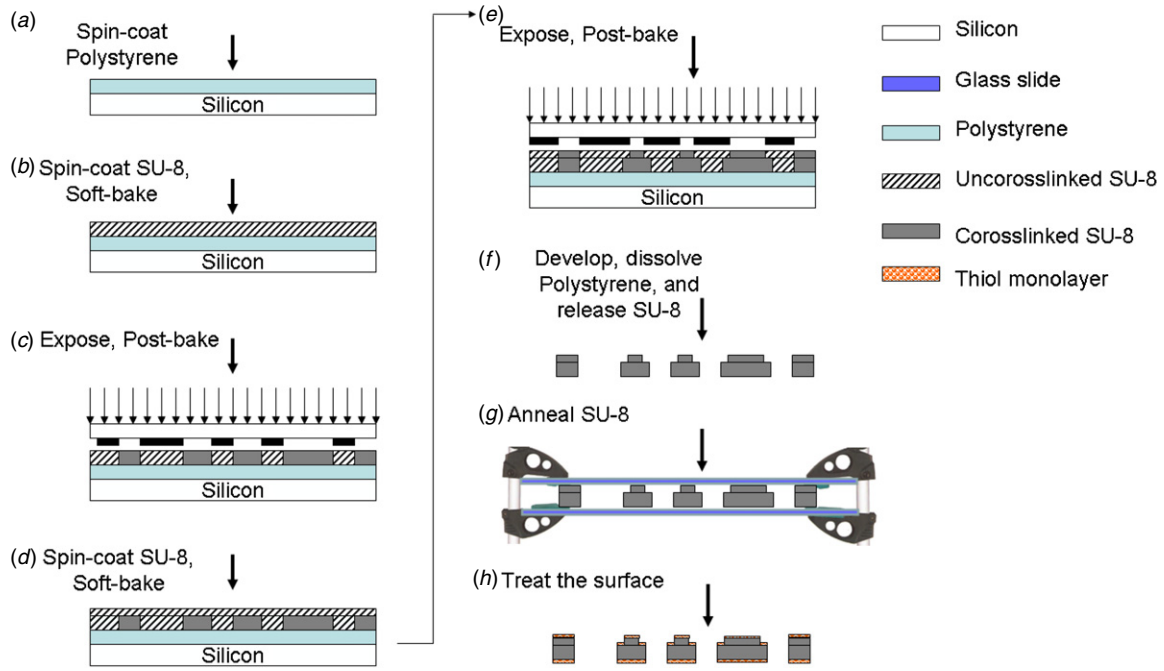


**Figure 3.** Schematic illustration of the fabrication process of SU-8 pins. (*a*) A solution of polystyrene dissolved in toluene is spin-coated on the substrate (3–4 $\mu$m thick) to serve as an adaptive release layer. (*b*) A layer of SU-8 is spin-coated and soft-baked. (*c*) The SU-8 is exposed to UV through a photomask and post-baked. (*d*) and (*e*) A second layer of SU-8 is spin-coated over the first layer and processed identically to the first one. (*f*) The SU-8 is developed and the polystyrene is dissolved using toluene to release the patterned SU-8 pins. (*g*) The pins are then clamped between two glass slides and annealed at 150 °C for 24 h to fully cross-link the SU-8, while minimizing internal stress. (*h*) Finally, the pin is coated with Au and the surface is patterned with hydrophobic (outside) and hydrophilic (inside) thiols.

### *2.3. Stop valve*

To minimize the variation of spot size and volume during spotting, it is important that the capillary pressure remains constant during the entire printing process. A pin with a straight conduit that stops at once (i.e. a dead-end channel) would satisfy the capillary pressure condition; however, because the conduit is open, dewetting of the liquid at the 'dead-end' is energetically unfavorable and the liquid column would dewet somewhere along the path and the liquid remains trapped in the pin at the dead-end. It is therefore important to include a stop valve in the flow path that stops the liquid from reaching the end of the slit, and design the valve such that it constitutes the location offering the least resistance to the draining of the liquid. Existing pins typically use graded enlargement of the channel width at the end of the capillary, which gradually increases the width to depth aspect ratio until filling becomes unfavorable. Because of the graded change, there is no definite stop, which in turn can lead to initial variability when starting to spot [17]. Stop valves can be formed by a sudden enlargement of a microfluidic conduit. When operating in a closed microchannel, it is difficult to make an efficient stop valve, because although the width can easily be enlarged, it is challenging to enlarge the depth simultaneously [24]. In the case of a pin, however, there are no bottom and top walls, and very robust valves can be produced that reliably stop a solution, even for highly wetting liquids [24–27].

## 3. Materials and methods

### *3.1. Microfabrication of the pins*

We fabricated one- and two-layer SU-8 pins using standard microfabrication procedures (figure 3 (for one-layer pins, steps (*d*) and (*e*) were skipped). First we crushed a polystyrene Petri dish (Fisher Scientific, Canada) and dissolved 10 g of polystyrene chips in 100 ml of toluene (Fisher Scientific, Canada) by stirring the solution at 80 °C for 5 h. We then poured 5 ml of the solution on a 4 in Si wafer and spin-coated the substrate at the rate of 3000 rpm for 30 s to form a 3–4 $\mu$m thick polystyrene layer. Subsequently, we placed the silicon wafer on a hotplate at 80 °C for 5 min to remove the solvent. The thin layer of polystyrene fulfills two functions. Firstly, it helps minimize the residual stress in the SU-8, and secondly, it serves as a sacrificial layer that facilitates the release of the pins from the substrate [9]. We patterned two layers of SU-8 using standard photolithography process atop the polystyrene layer. The parameters of the baking steps used to make the SU-8 pins are summarized in table 1. We then developed the microstructures of both layers at once by immersing the wafer in the SU-8 developer (propylene glycol methyl ether acetate, Microchem, USA), which was followed by the release of the SU-8. The wafer was immersed in a toluene bath for 5–10 min and gently agitated until the layer detached from the substrate. The pins were characterized by both optical (LV150 industrial microscope, Nikon, Japan) and scanning electron microscopy (S-3000N variable pressure SEM, Hitachi, Japan).

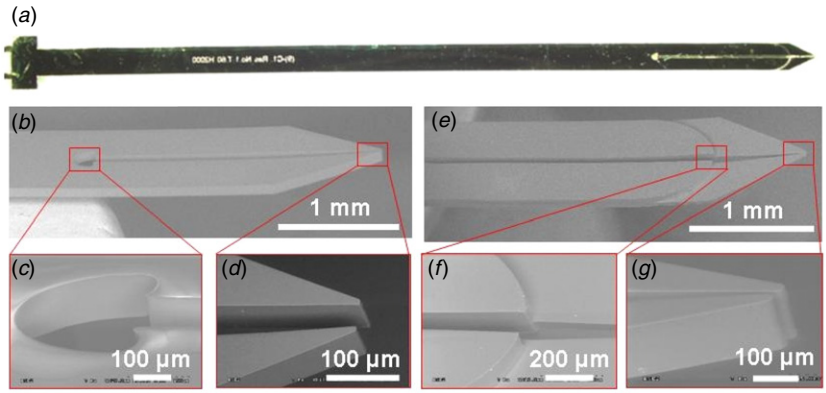


**Figure 4.** Micrographs of microfabricated SU-8 pins. (*a*) Overview of a pin coated with Au. The pattern in the middle of the pin is a label that was structured into each pin. The 7 mm long, 100 $\mu$m wide slit is visible at the right. (*b*) SEM image showing the entire slit and tip of a single-layer, 200 $\mu$m thick tip along with close-up views of (*c*) the stop valve and (*d*) the tip. (*e*) SEM of a double-layer pin, (*f*) the interface of the two layers and (*g*) the 75 $\mu$m thick tip.

**Table 1.** SU-8 processing parameters.

| | Obtained thickness ($\mu$m) | Soft bake | Exposure energy (mJ cm$^{-2}$) | Post-exposure bake (heating) | Post-exposure bake (cooling) |
|---|---|---|---|---|---|
| First layer | 75 | 5 min at 65 °C and 25 min at 90 °C | 200 | From 20 to 70 °C at 0.5 °C/min; keep at 70 °C for 30 min | From 70 to 20 °C at 0.5 °C/min |
| Second layer | 100 | 5 min at 50 °C and 45 min at 70 °C | 230 | From 20 to 70 °C at 0.5 °C/min; keep at 70 °C for 30 min | From 70 to 20 °C at 0.5 °C/min |

### *3.2. Annealing of SU-8 to eliminate the residual stress*

We developed an annealing process to remove the residual stress in SU-8. The freestanding pins were clamped between two rigid glass slides (75 × 25 × 1 mm$^3$ microscope slides, Fisher Scientific, Canada) by using paper clips (fold back clips, Staples, Canada; see figure 3(*g*)). Using a programmable oven (Lindberg Blue M, Fisher Scientific, Canada), we subjected the setup to a heat cycle which consisted of first a temperature ramp from room temperature to 150 °C in 15 h, then keeping it constant at 150 °C for 15 h and finally cooling it down to room temperature in 24 h.

### *3.3. Surface treatment of the pins*

We coated the pins by sputtering 10 nm Ti followed by 50 nm of Au. Then we used a flat stamp of poly(dimethylsiloxane) (PDMS; Sylgard 184, Dow Corning) inked with a solution of 1% *n*-decanethiol (Fluka, Canada) in ethanol to print on the top- and back-side surface of the pin to coat the outer surfaces with a hydrophobic *n*-decanethiol [22]. The slit of the pins was then selectively coated with hydrophilic tihols by immersing them for 1 h in a 1 mM solution of PEG-thiol (Rapp Polymere, Germany) in water. Figure S3 in the supplementary materials, available at stacks.iop.org/JMM/20/055001/mmedia, illustrates the entire patterning process.

### *3.4. Spotting and imaging of proteins*

We first placed the pins in a commercial pin-holder (Parallel Synthesis, USA) with two micromachined collimators (see figure S4 in the supplementary materials, available at stacks.iop.org/JMM/20/055001/mmedia, for more details), and spotted the microarray using a customized spotting robot (nano-plotter 2.0, Gesim, Germany). Chicken antigoat IgG, labeled with fluorescein, was diluted at a concentration of 200 $\mu$g ml$^{-1}$ in a solution of carbonate buffer at pH 9 containing 10% glycerol. The solution was spotted with a single pin on an epoxy-coated glass slide (Nexterion, Schott, USA). The slide with the array of droplets forming the protein array was scanned with a laser scanner (LS400, Tecan, NC, USA) using 532 nm laser and a resolution of 10 $\mu$m. The images were analyzed using Image J.

## 4. Results and discussions

### *4.1. Fabrication*

Two variants of the pins were fabricated using either one or two layers of SU-8, but always with a total thickness of 200 $\mu$m so as to fit into the collimator (see figure 1). Figure 4 shows micrographs of both types of pins. The single-layer SU-8 pins made using only one lithographic exposure had a slit with a width of 50 $\mu$m and a total width of 75 $\mu$m at the tip. Two-layer pins were fabricated using two-step lithography process with a tip size of 50 × 75 $\mu$m$^2$ and therefore lead to much smaller spots.

The volumetric capacity of the pins was adjusted by making channels with different lengths, and by making pins with two channels (see figure S5 in the supplementary materials,

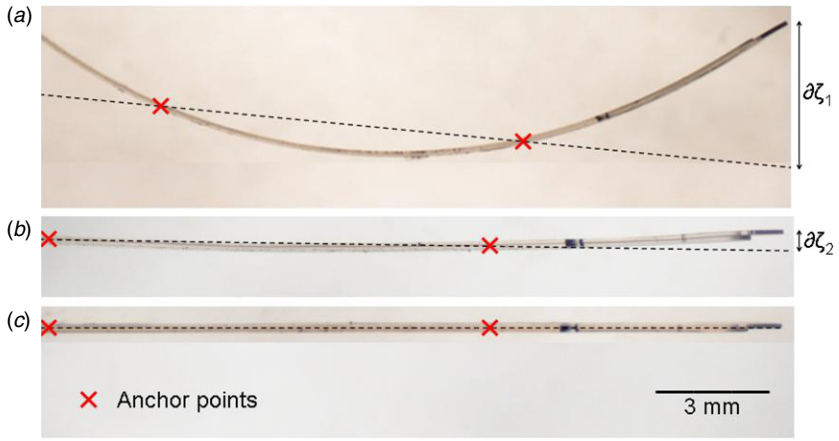


**Figure 5.** Visualization and quantification of the deflection $\partial\zeta$ of 200 $\mu$m thick SU-8 pins seen lying on their side and that were fabricated using different processes described in the text. $\partial\zeta$ is defined as the deflection of a pin at the tip when fixed by the two anchor points of a collimator marked by an X. (*a*) Pin fabricated according to the recipe recommended by the manufacturer, which leads to a deflection of $\partial\zeta_1 \approx 6$ mm. (*b*) Pin made using optimized baking parameters and an adaptive polystyrene layer, $\partial\zeta_2 = 500 \pm 200$ $\mu$m. (*c*) Pin fabricated with the same recipe as in (*b*), and subjected to an annealing step, $\partial\zeta_3 = 0 \pm 30$ $\mu$m.

available at stacks.iop.org/JMM/20/055001/mmedia, for additional details). The pins presented here have a transfer capacity of 100–300 nl.

### *4.2. Annealing process*

A critical parameter for pin spotting is the alignment and straightness of the pins. Indeed, high-density arrays have a pitch of only 250 $\mu$m, which implies that the pins need to be perfectly straight as a deviation of even a few hundred micrometers (for a length of 30 mm) can lead to an overlap of adjacent spots. Bending of the SU-8 structures is caused by the internal stress, arisen as a consequence of the thermal mismatch and the asymmetric configuration of the SU-8 atop of the Si wafer during the post-baking process. So the requirements for thin, slender and straight pins represent a major challenge for SU-8 pins [13].

To quantify the deflection of the pins due to the residual stress, we introduce a deflection variable $\partial\zeta$, which is defined as the deflection of the pin, once it is placed between the two anchor points in the pin collimators used for spotting. Figure 5(*a*) shows the deflection of an SU-8 pin that was spin-coated directly on a sacrificial layer of polystyrene and processed according to recipes of the manufacturer [12]. As can be seen, the pin is strongly bent and deflects $\partial\zeta \approx 6$ mm.

With optimized baking parameters and by using an adaptive polystyrene layer (as described in table 1), the deflection could be decreased to $\partial\zeta = 500 \pm 200$ $\mu$m (see figure 5(*b*)). The value $\pm 200$ $\mu$m corresponds to the maximal variability observed among different pins. The residual stress of the pin can be approximated as [28]

$$\sigma_{\max} = -\frac{Et}{2\rho} \tag{4.1}$$

where $\rho$ is the radius of the curvature, $\sigma_{\max}$ is the maximum residual stress, $E$ is the elastic Young's modulus of SU-8 and $t$ is the thickness of the pin.

$\partial\zeta \approx 500 \pm 200$ $\mu$m corresponds to $\rho = 172 \pm 68$ mm (see figure S6 in the supplementary materials, available at stacks.iop.org/JMM/20/055001/mmedia, for more details). Substituting into equation (4.1) the maximum residual stress in the pin after optimizing the baking parameters is found to be $\sigma_{\max} = 33.4 \pm 13.4$ MPa, which is within the range of stress values reported in the literature [11, 12].

SU-8 shrinks 6–10% during the cross-linking and post-baking processes [11, 29], which is a great source of stress, and makes it difficult to find a substrate that follows the same expansion cycles during post-bake and subsequent thermal cooling of the SU-8. However, we reasoned that by having a symmetric setup—achieved by clamping the SU-8 structure between two identical substrates—the asymmetric stress buildup arising when a single substrate is used could be reduced. An additional annealing step was therefore introduced at a temperature of 150 °C using two glass slides to clamp the pins (see figure 3(*g*)). Since the SU-8 glass transition temperature is around 175 °C [30], we found that when annealing with 175 °C or more, the tips of the pins were stuck to one another after processing. By reducing the annealing temperature to 150 °C, the tips remained separate while still minimizing the stress. We also found that slow ramping, and in particular, slow cooling further helped reducing the residual bending. When using the set of optimized parameters presented in section 4.2, the residual bending of SU-8 was reduced within the accuracy of the optical measurements used, $\partial\zeta = 0 \pm 30$ $\mu$m (see figure 5(*c*)). Here, the value $\pm 30$ $\mu$m corresponds to the estimated accuracy of our imaging setup. We also found that annealed pins were stable for at least 10 months, figure 5(*c*), whereas non-annealed pins tend to bend after a few weeks up to $\partial\zeta = 2000 \pm 1400$ $\mu$m (figure is not shown), which we attribute to the evaporation of the residual solvent.

### *4.3. Toughness and flexibility of the polymer pins*

Polymers are tougher and more flexible than Si, which should translate into more reliable pins. Indeed, Si pins regularly break due to the brittleness of Si. To illustrate


**Figure 6.** Images extracted from a movie showing the elastic buckling of an SU-8 pin as it is being pressed against a substrate, followed by its unbending. (*a*) The SU-8 pin before elastic deformation, (*b*) and (*c*) during elastic buckling, and (*d*) after buckling.

the resilience of the SU-8 pins, they were subjected to a bending cycle (see figure 6, showing how the pin buckles without breaking and flexes back to its original shape (also see the movie S1 in the supplementary materials, available at stacks.iop.org/JMM/20/055001/mmedia). The tip of the pin did not show any visible deterioration (data not shown). Although such high loads are not normally applied during microarray spotting, software glitches and human errors sometimes result in pins being subjected to high strain, which often lead to the destruction of metal or Si pins. In the course of a printing experiment described below, a pin was subjected to 2000 buckling cycles, as shown in figure 6 without observing notable permanent deformation for the pin or the tip.

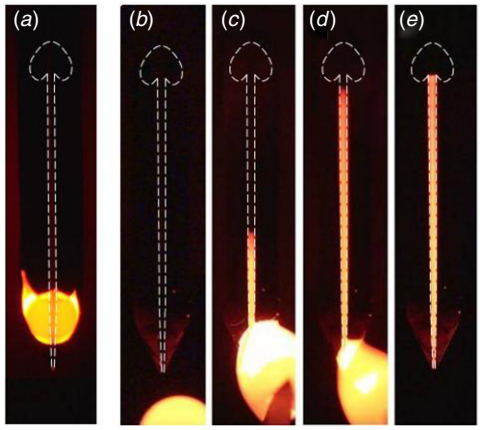


**Figure 7.** Capillary filling of pins. (*a*) Fluorescence micrograph of an SU-8 pin without surface treatment that was dipped into a solution containing fluorescent rhodamine. (*b*) Pin coated with a hydrophobic thiol on the outside and a hydrophilic PEG-thiol on the inside. (*c*) Upon contacting a droplet, (*d*) the liquid spontaneously fills the slit. (*e*) The bubble with the stop valve stops the filling and ensures precise metering of the solution within the pin.

### *4.4. Surface treatment*

Native SU-8 is hydrophobic with $\theta_{\text{water-SU-8}} = 90^\circ$ [31] and therefore in the absence of surface treatment, aqueous solutions do not spontaneously fill the slit of the pin. Figure 7(*a*) shows a native SU-8 pin that was dipped into an aqueous solution containing fluorescent rhodamine dye. Whereas the slit was not filled, a drop was attached to the tip of the pin. To ensure spontaneous filling of the slit with water, the inside of the slit was selectively made hydrophilic using a self-assembled PEG-thiol monolayer. Following this treatment, the liquid spontaneously filled the slit and no drops attached to the outside of the pin (figure 7(*b*)–(*e*)) (see the movies S2 and S3 in the supplementary materials, available at stacks.iop.org/JMM/20/055001/mmedia). The surface treatment is critical to obtain functional pins and prevent droplets from attaching to the outer surfaces of the pins.

### *4.5. Spotting of proteins*

Pins were used to spot a solution with a fluorescently labeled protein as a microarray. Slides are commonly scanned after

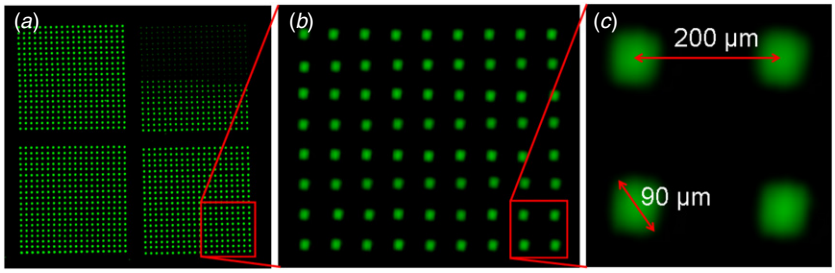


**Figure 8.** Fluorescence images of a microarray of 1392 spots of a fluorescent protein that were spotted using an SU-8 pin in one run with a pitch of 200 $\mu$m. (*a*) Overview of the array with 4 sub-arrays of 20 $\times$ 20 spots. The last visible well-printed spot is at the 12th row on the 10th line. (*b*) Close-up view of 8 $\times$ 9 spots and (*c*) four spots of the microarray.

washing only, the size and homogeneity of the spot can vary due to inhomogeneity of the surface chemistry. To avoid this problem, we scanned the slides immediately after spotting with an SU-8 pin 2000 times, while the droplets were still present on the glass slide. For the protein spotting, a two-layer pin with a tip size of $50 \times 75$ $\mu m^2$, and a 7 mm long slit with a capacity of 140 nl was used. The humidity was set at 70% and the solution contained 10% glycerol to further reduce evaporation, which allowed printing 1392 spots in a single run (see figure 8). The spots produced by this pin are 90 $\mu$m along the diagonal. The subsequent spots are barely visible, indicating that the sample was used up. Neglecting evaporation, the volume of each deposited spot is 100 pl, which is comparable to the volumes of liquid deposited by conventional pins or inkjet spotting. We found that the maximum size variation falls within the 10 $\mu$m resolution of the scanner for the first 1392 spots of the array. Further studies are needed to determine whether the attachment of proteins to the slide surface follows the same trends, which will be tested in future studies.

## 5. Conclusion

We have introduced SU-8 fabrication process that allows making stress-free, straight structures. The key to the successful fabrication of these pins was the development of an annealing step, which allows making 200 $\mu$m thin polymer structures that are 30 mm long and straight within 30 $\mu$m. Polymer pins with a novel stop valve design and surface chemical treatment served to illustrate some of the possibilities of this process. The functionality of the pins was demonstrated by mechanically loading and buckling them, and by printing 1392 spots with a constant diameter of 90 $\mu$m using a single filling. These pins are made by a two-step standard lithography process without need for complicated equipment beyond a mask aligner, hot plates and an oven for annealing. The capital investment needed for microfabricating SU-8 pins is much smaller when compared to Si pins, for example, which require a deep reactive ion etcher. In addition, the material costs are low as well, since no more than 10 ml of SU-8 are used for making 100 pins, which corresponds to a material cost of less than 10 cents per pin. SU-8 thus represents a robust and low-cost alternative for making microarray spotting pins.

The fabrication process outlined here may be applied to any flat, freestanding patterned polymer structure made of SU-8. We foresee that it may, for instance, be used to fabricate neuronal probes for invasive recording in the brain, which need to be straight and flexible [32]. In addition, the strategy outlined here may also be applied to molded thermoplasts such as poly(methyl methacrylate), polystyrene, polycarbonate, cyclic-polyolefin copolymer, etc, because residual stress also builds up as a result of thermal gradients and asymmetric shrinkage of structures [33]. The concept of symmetrical heating and cooling may be adapted to polymer features that remain (partially) attached to a substrate. By using two identical substrates to clamp the polymer, asymmetrical stress buildup following thermal cycling can be prevented by using a perfectly symmetrical setup.

## Acknowledgments

We would like to acknowledge funding from NSERC, CIHR, CHRP, Genome Canada, Genome Quebec, CFI, and the assistance of the McGill Nanotools Microfab Laboratory (funded by CFI, NSERC and VRQ). DJ acknowledges support from a Canada Research Chair. MAQ acknowledges an Alexander Graham Bell Canada Graduate NSERC Scholarship. MPR acknowledges financial support from the Spanish Ministry of Science through a post-doctoral fellowship.

## References

[1] Liu G, Tian Y and Kan Y 2005 Fabrication of high-aspect-ratio microstructures using SU8 photoresist *J. Microsyst. Technol.* **11** 343–6
[2] Nordstrom M *et al* 2008 SU-8 cantilevers for bio/chemical sensing: fabrication, characterisation and development of novel read-out methods *Sensors* **8** 1595–612
[3] Backmann N *et al* 2005 A label-free immunosensor array using single-chain antibody fragments *Proc. Natl Acad. Sci. USA* **102** 14587–92
[4] Abgrall P *et al* 2007 SU-8 as a structural material for labs-on-chips and microelectromechanical systems *Electrophoresis* **28** 4539–51
[5] Ruano-Lopez J M *et al* 2009 The SmartBioPhone™, a point of care vision under development through two European projects: OPTOLABCARD and LABONFOIL *Lab Chip* **9** 1495–9
[6] Ezkerra A *et al* 2007 Fabrication of SU-8 free-standing structures embedded in microchannels for microfluidic control *J. Micromech. Microeng.* **17** 2264–71
[7] Bystrova S, Luttge R and Van Den Berg A 2007 Study of crack formation in high-aspect ratio SU-8 structures on silicon *J. Microelectron. Eng.* **84** 1113–6
[8] Abgrall P *et al* 2008 Low-stress fabrication of 3D polymer free standing structures using lamination of photosensitive films *J. Microsyst. Technol.* **14** 1205–14
[9] Luo C *et al* 2004 Releasing SU-8 structures using polystyrene as a sacrificial material *Sensors Actuators* A **114** 123–8
[10] Foulds I G, Johnstone R and Parameswaran M 2008 Polydimethylglutarimide (PMGI) as a sacrificial material for SU-8 surface-micromachining *J. Micromech. Microeng.* **18** 075011
[11] Conedera V *et al* 2007 Surface micromachining technology with two SU-8 structural layers and sol–gel, SU-8 or $SiO_2$/sol–gel sacrificial layers *J. Micromech. Microeng.* **17** N52–7
[12] Hammacher J *et al* 2008 Stress engineering and mechanical properties of SU-8-layers for mechanical applications *J. Microsyst. Technol.* **14** 1515–23
[13] Keller S *et al* 2008 Processing of thin SU-8 films *J. Micromech. Microeng.* **18** 125020
[14] Barbulovic-Nad I *et al* 2006 Bio-microarray fabrication techniques—a review *Crit. Rev. Biotechnol.* **26** 237–59
[15] Schena M *et al* 1995 Quantitative monitoring of gene-expression patterns with complementary-DNA microarray *Science* **270** 467–70
[16] Kambhampati D 2005 *Protein Microarray Technology* (Weinheim: Wiley-VCH) chapter 2
[17] Parallel Synthesis Co. (retrieved December 2008) http://www.parallel-synthesis.com/
[18] Rose D, and Tisone T C 1999 Tip design and random access array for microfluidic transfer *US Patent* 6551557
[19] George R A, Woolley J P and Spellman P T 2001 Ceramic capillaries for use in microarray fabrication *J. Genome Res.* **11** 1780–3

[20] Schena M (ed) 2000 *Microarray Biochip Technology* 1st edn (Sunnyvale, CA: Eaton Publishing) chapter 9
[21] Bruus H 2008 *Theoretical Microfluidics* 1st edn (Oxford: Oxford University Press) chapter 7
[22] Juncker D *et al* 2002 Autonomous microfluidic capillary system *J. Anal. Chem.* **74** 6139–44
[23] Al-Halhouji A T *et al* 2008 Nanoindentation testing of SU-8 photoresist mechanical properties *J. Microelectron. Eng.* **85** 942–4
[24] Zimmermann M, Hunziker P and Delamarche E 2008 Valves for autonomous capillary systems *Microfluid. Nanofluid.* **5** 395–402
[25] Melin J *et al* 2004 A liquid-triggered liquid microvalve for on-chip flow control *Sensors Actuators* B **100** 463–8
[26] Chen J M, Huang P C and Lin M G 2008 Analysis and experiment of capillary valves for microfluidics on a rotating disk *Microfluid. Nanofluid.* **4** 427–37
[27] Leu T S and Chang P Y 2004 Pressure barrier of capillary stop valves in micro sample separators *Sensors Actuators* A **115** 508–15
[28] Beer F P, Johnston J and Dewolf J T 2008 *Mechanics of Materials* 7th edn (New York: McGraw Hill) chapter 3
[29] Chung C K and Hong Y Z 2007 Surface modification of SU8 photoresist for shrinkage improvement in a monolithic MEMS microstructure *J. Micromech. Microeng.* **17** 207–12
[30] Serra S G *et al* 2007 A simple bonding process of SU-8 to glass to seal a microfluidic device *Proc. 3rd Int. Conf. on Multi-Material Micro Manufacture (Borovets, Bulgaria, 3–5 October 2007)* (Dunbeath: Whittles) pp 43–6
[31] Nordstrom M *et al* 2004 Rendering SU-8 hydrophilic to facilitate use in micro channel fabrication *J. Micromech. Microeng.* **14** 1614–7
[32] Hajj-Hassan M, Chodavarapu V P and Musallam S 2009 Microfabrication of ultra-long reinforced silicon neural electrodes *Micro Nano Lett.* **4** 53–8
[33] Malek C K *et al* 2007 Revisiting micro hot-embossing with moulds in non-conventional materials *J. Microsyst. Technol.* **13** 475–81

# SUPPLEMETARY MATERIALS

## COMMERCIAL PIN HOLDER WITH COLLIMATOR

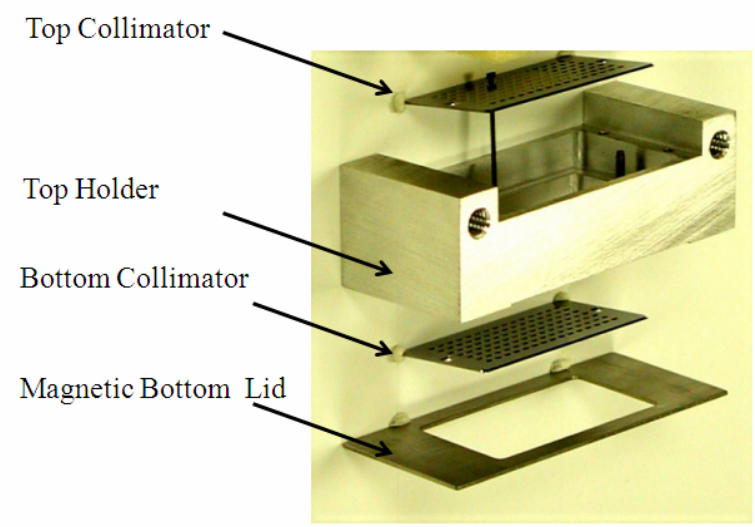


**Figure S1** A disassembled view of the pin holder. Courtesy of Parallel synthesis Technologies Inc. [1]

## MECHANICAL STABILITY OF THE PINS UNDER APPLIED CAPILLARY PRESSURE

To approximate the tip deflection of these pins due to the capillary force, the stress analysis was performed by a finite element calculation of the set of partial differential equations (PDEs) for the system geometry using a commercially available modeling package [2]. The capillary force was applied as a distributed pressure on the microchannel, which can be calculated as:

$$P = +\frac{2\gamma}{t} - \frac{2\gamma\cos\theta_r}{w}, \tag{S.1}$$

where $w$ is the width of the channel, and $\theta_r = 30^\circ$ is the receding contact angle between liquid and the surface [3]. Tetrahedral elements were used to mesh the geometry. 570000 and 1800000 elements were used to approximate the displacement. No substantial changes were observed in the calculated results. So the finer mesh was used as the approximated value. Figure S1 illustrates the results. It can be observed that for the SU-8 pins, the deformation in the tip due to the capillary pressure is less than 1μm for the case where the length of the microchannels is 7000 μm.

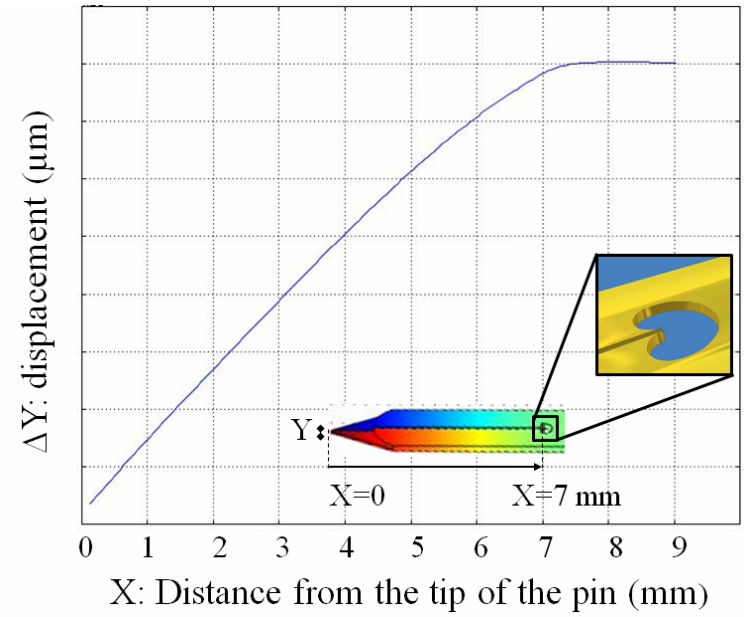


**Figure S2.** The effect of the capillary pressure on the elastic deformation of the microchannel in the polymer pins. Comsol multiphysics 3.4 was used to approximate the deformation. The modeling is for the case where the length of the microchannel is 7000 μm. The maximum deflection is less than 2% of the size of the tip (i.e. 1 μm over 60 μm tip size )

## SURFACE TREATMENT OF THE PINS

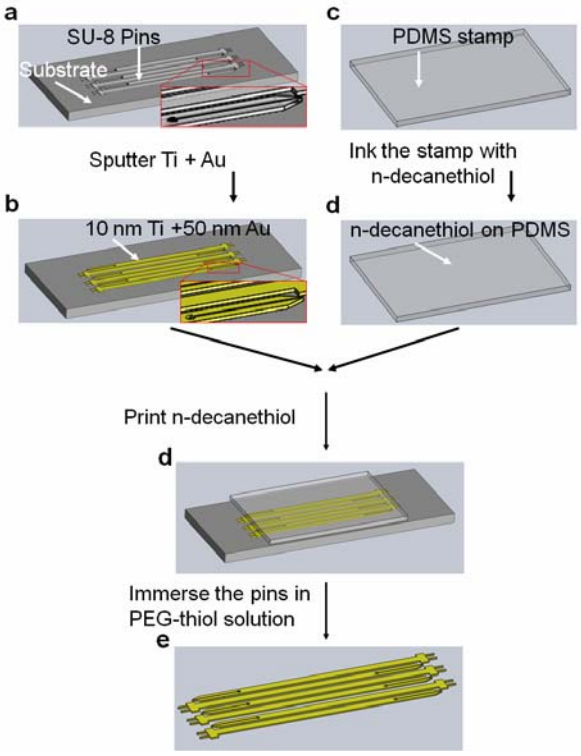


**Figure S3** Surface treatment of the SU-8 pins. (a) 10 nm of Titanium and 50 nm of Gold were sputtered on the SU-8 pins. (b) To coat the PDMS stamp with a thin layer of n-decanethiol, the stamp was inked with a diluted solution of n-

decanethiol in ethanol and blow dried. (c) In order to make the outer surface hydrophobic the gold coated pins were printed with thiol. (d) The pins were immersed in the dilute solution of PEG thiol in water to make the µchannels hydrophilic.

## PINS MOUNTED IN A CUSTOMIZED INK-JET SPOTTER

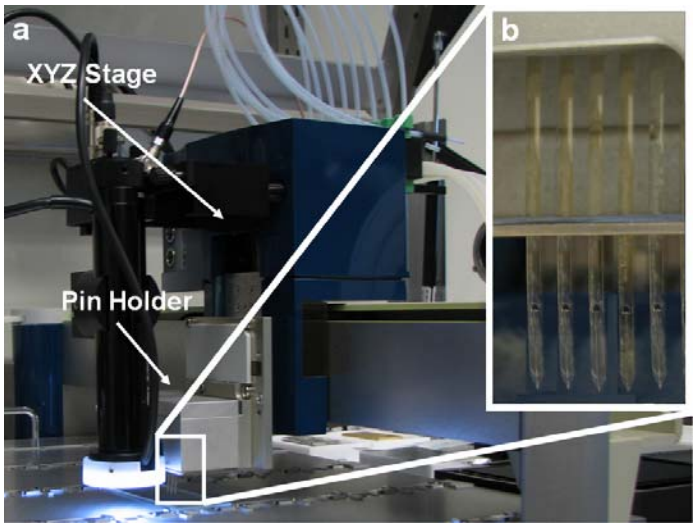


**Figure S4.** Customized ink-jet spotter. (a) Images of the pins mounted in a customized pin spotter (Nanoplotter 2.0, Gesim, Germany). (b) Close-up view of the pins mounted in the holder

## TWO CHANNEL PINS

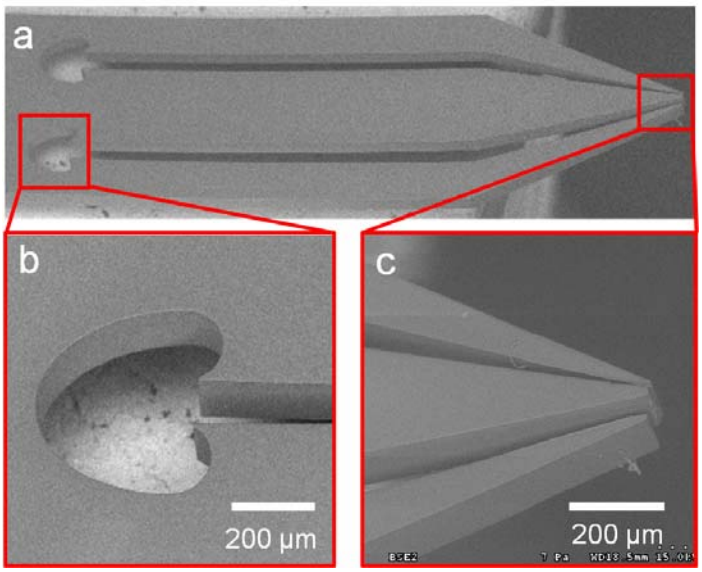


**Figure S5.** SEM images of the two channel pins to transfer larger amount of liquids. (a) Two channel pins. (b) Enlarged view of the stop valve. (c) Enlarged view of the tip of the pin.

## RESIDUAL STRESS MEASUREMENT

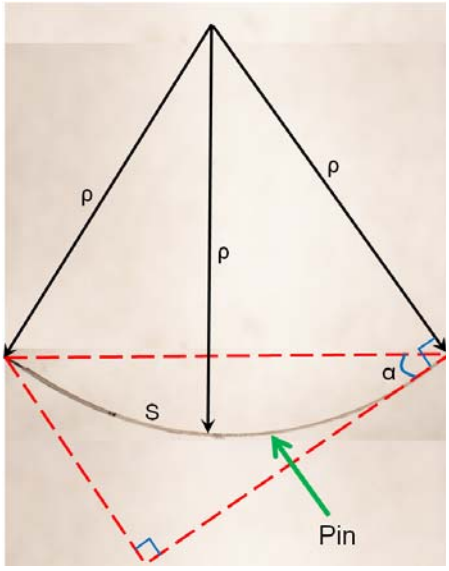


**Figure S6.** Approximating α with respect to ρ, the radius of the curvature of the pin, and *S*, the length of the pin

$$\rho = \frac{S}{2\alpha} \tag{S.2}$$

Where $S$ is the length of the curvature, which is 30 mm, and α is an angel between the tangent line to the curvature and a line connecting the two ends of the pin.

## REFERENCES


[1] "Parallel Synthesis Technologies Inc. ," 2009-08-27; http://www.parallel-synthesis.com.

[2] A. A. M. Morales, G. Nunez-Gandolff, N. P. Perez *et al.*, "Freeze-dried formulation for direct Tc-99m-labeling ior-egf/r3 MAb: Additives, biodistribution, and stability," *Nuclear Medicine and Biology,* vol. 26, no. 6, pp. 717-723, 1999.

[3] D. Juncker, H. Schmid, U. Drechsler *et al.*, "Autonomous microfluidic capillary system," *Analytical Chemistry,* vol. 74, no. 24, pp. 6139-6144, 2002.